

# 19<sup>th</sup> Patras Workshop on Axions, WIMPs and WISPs

Marios Maroudas

Working Group: D. Horns, M. Maroudas, L. H. Nguyen, Z. Zhang

---

## Dark Matter searches with WISPLC experiment



# Theoretical Background

- In the presence of axions, Maxwell's equations are modified as [4]:

$$\begin{aligned}\nabla \cdot \mathbf{E} &= g\mathbf{B} \cdot \nabla a + \rho_{el} \\ \nabla \times \mathbf{B} - \frac{\partial \mathbf{E}}{\partial t} &= g_{a\gamma\gamma} \left( \mathbf{E} \times \nabla a - \mathbf{B} \frac{\partial a}{\partial t} \right) + \mathbf{j}_{el}\end{aligned}$$

- For  $m_a \sim \text{neV}$ , axion behaves as a coherent oscillating scalar field ( $\lambda \sim 10^5 \text{ m}$ ):

$$a(t) = a_0 \cos(m_a t) = \frac{\sqrt{2\rho_{DM}}}{m_a} \cos(m_a t)$$

- An external B-field induces an axion sourced current density oscillating at the Compton freq. of axions:

$$\mathbf{j}_a(t) = -g_{a\gamma\gamma} \mathbf{B} \frac{\partial a}{\partial t}$$

- This generates an oscillating perpendicular toroidal magnetic field such that:  $\nabla \times \mathbf{B}_a = \mathbf{j}_a$

# Detection Scheme – WISPLC

- External  $\mathbf{B}_0$ - field converts axions to an oscillating displacement current  $\mathbf{j}_a$ :

$$\mathbf{j}_a = -g_{a\gamma\gamma} \mathbf{B}_0 \frac{\partial a}{\partial t} = g_{a\gamma\gamma} \sqrt{2\rho_{DM}} \mathbf{B}_0 \sin(m_a t)$$

- The oscillating current induces a toroidal magnetic field  $\mathbf{B}_a \perp \mathbf{j}_a$ :

$$\mathbf{B}_a = g_{a\gamma\gamma} \sqrt{2\rho_{DM}} \sin(m_a t) \int \frac{\mathbf{B}_0 \times (\mathbf{r} - \mathbf{r}')}{|\mathbf{r} - \mathbf{r}'|^3} dV$$

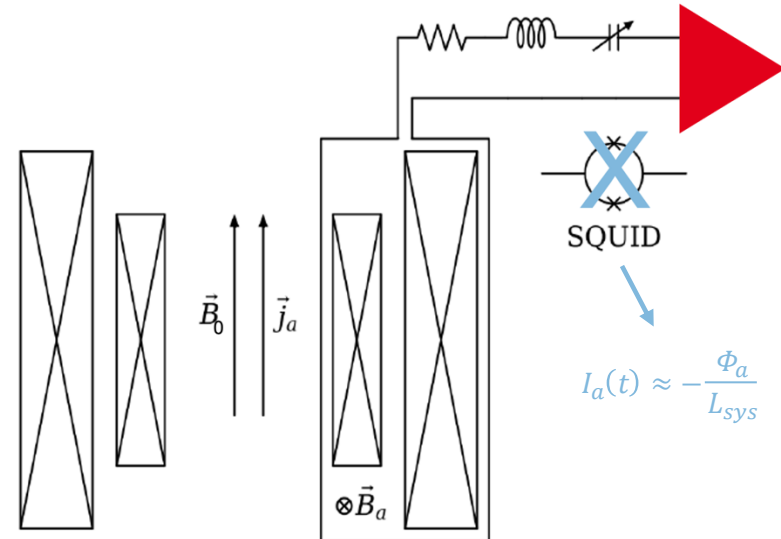
$$\Phi_a = g_{a\gamma\gamma} \sqrt{2\rho_{DM}} \sin(m_a t) \int_{loop} dA \int \frac{\mathbf{B}_0 \times (\mathbf{r} - \mathbf{r}')}{|\mathbf{r} - \mathbf{r}'|^3} dV \cdot \hat{\mathbf{n}}_{loop}$$

- The toroidal magnetic field creates an AC EMF =  $-d\Phi_a/dt$ .
- EMF induces a voltage in a pickup loop (with N windings):

$$V_a(t) = N \cdot \frac{d\Phi_a(t)}{dt}$$

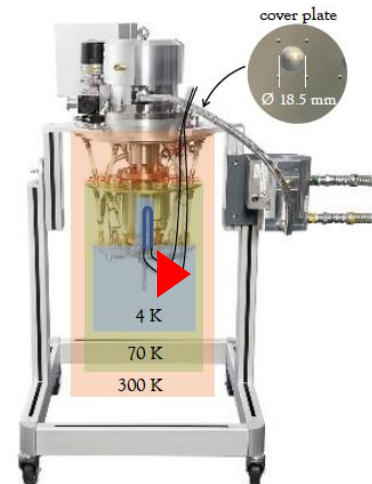
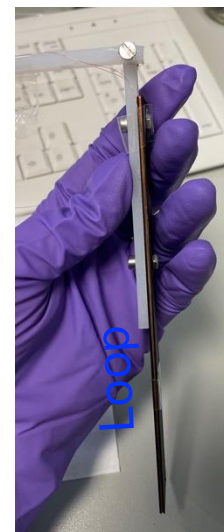
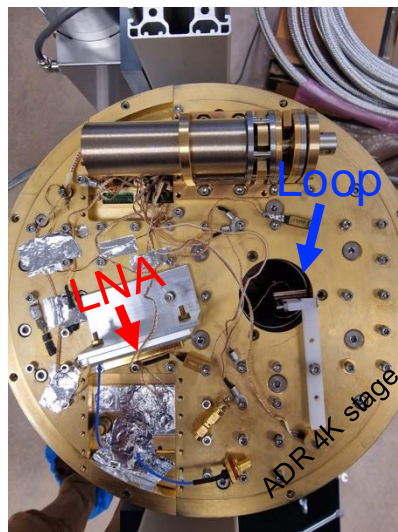
- An LC circuit can tune and resonantly enhance the expected signal by Q at  $\omega = \frac{1}{\sqrt{LC}}$ .

- WISPLC [5] employs **voltage detection** instead of **current** using a **LNA** instead of a **SQUID**.
- Axion mass / frequency-dependent sensitivity!**



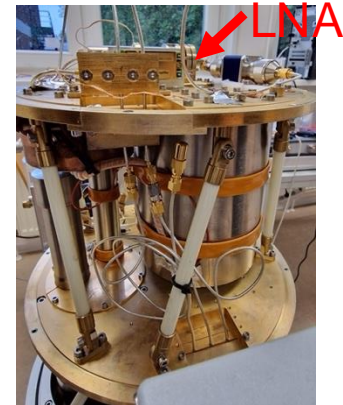
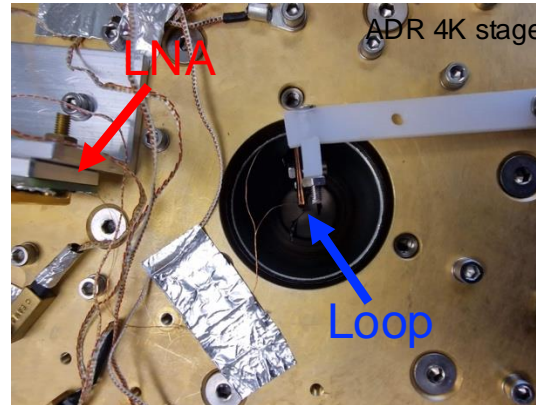
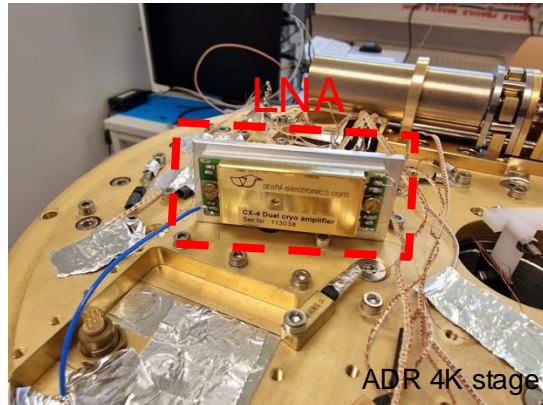
## WISPLC Prototype – Setup (Broadband Case)

- A **250 cm** pickup **loop** from **0.1 mm Cu** wire is used wound 7 times around a rectangular 16 x 2 cm PTFE holder.
- The **loop** is placed inside the bore of a dipole **6 T** magnet of an ADR parallel to the magnetic field.
- Loop connected to a high-input impedance Stahl CX4 **LNA** providing **~67 dB** amplification @ 4K with a noise temperature **< 1K**.
- Post-amplification of ~40 dB via a room-temp Femto HSA LNA and **readout through an SPCM ADC**.



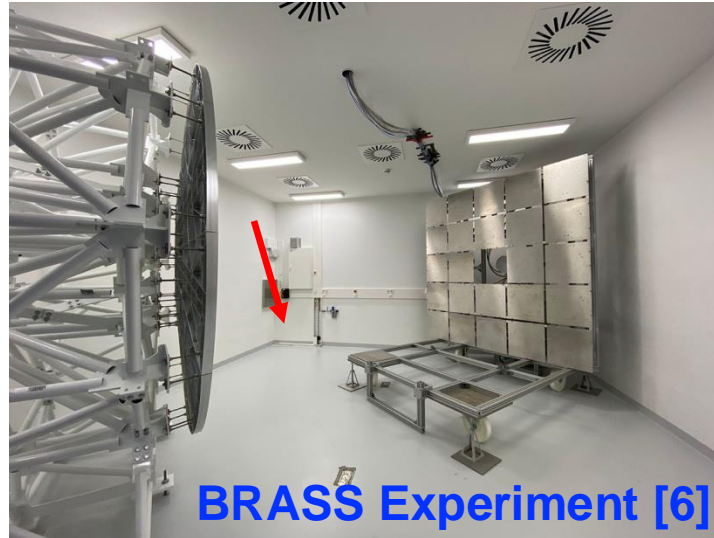
# WISPLC Prototype – LNA

- SQUID magnetometers are very sensitive to stray magnetic fields in comparison to HEMTs
- LNA has M $\Omega$  input resistance to reject current noise so only the voltage is amplified.
- LNA mounted with optimum orientation to the stray static magnetic field.

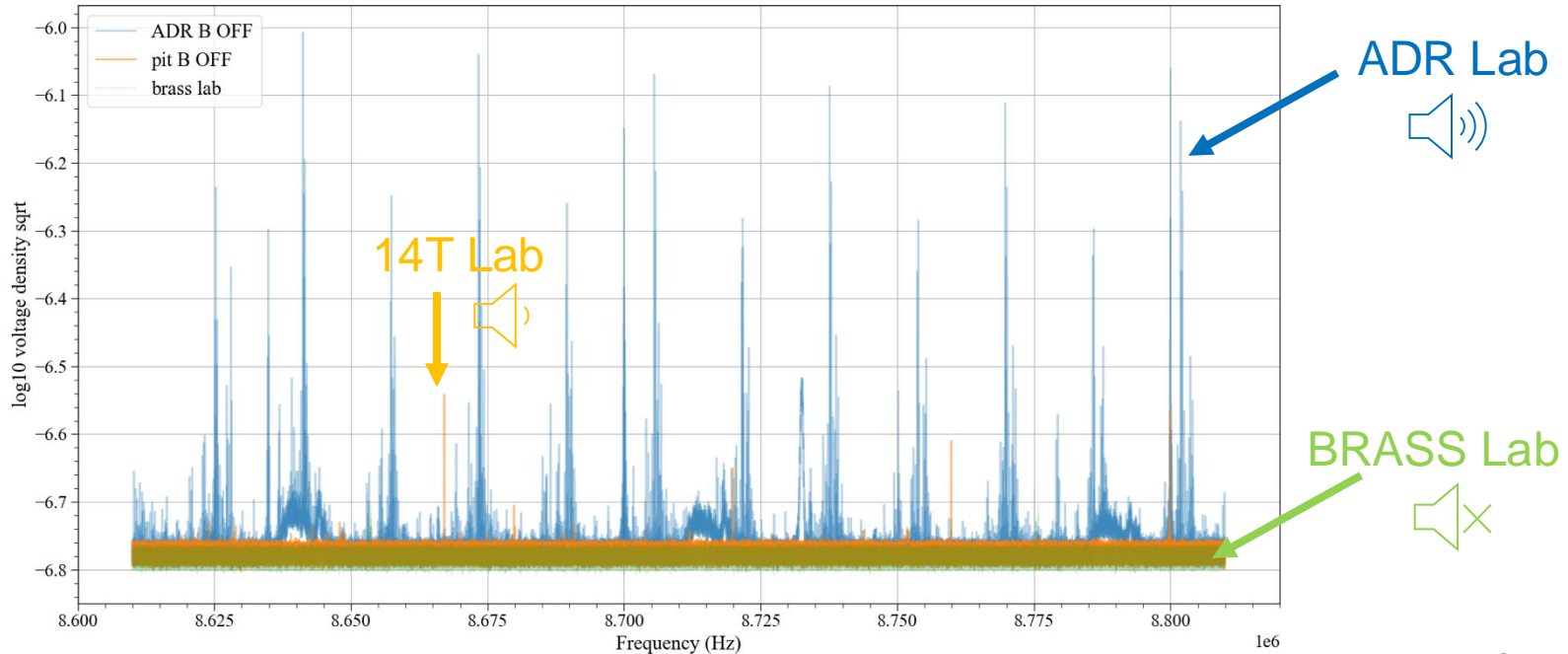


## WISPLC Prototype – Shielding

- Setup installed inside the **radiation-shielded BRASS lab** [6] to reduce external EMI/EMC parasites.
- Compressors, chillers and control/monitoring rack placed outside.



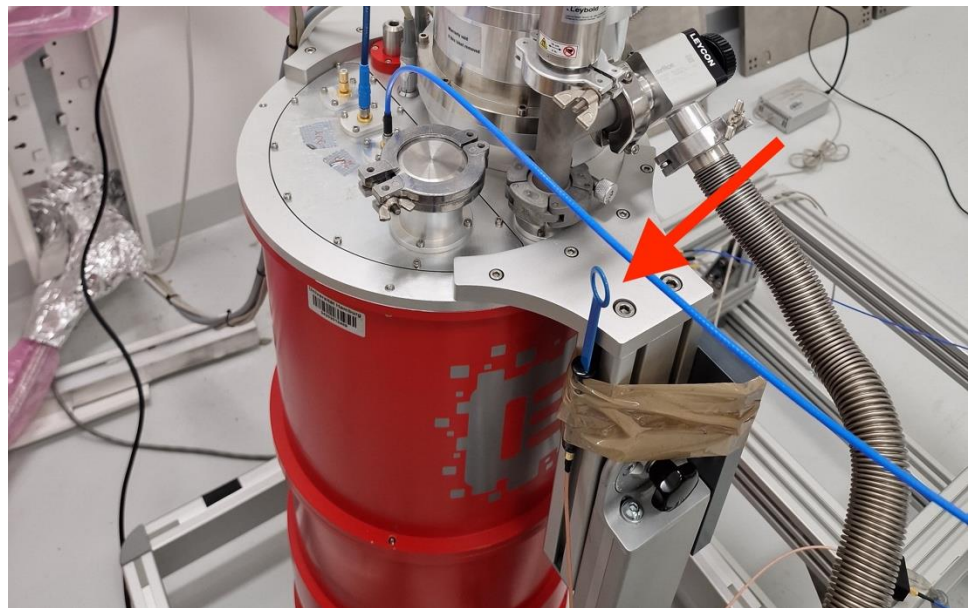
# WISPLC Prototype – Shielding



## WISPLC Prototype – EMI/EMC Identification

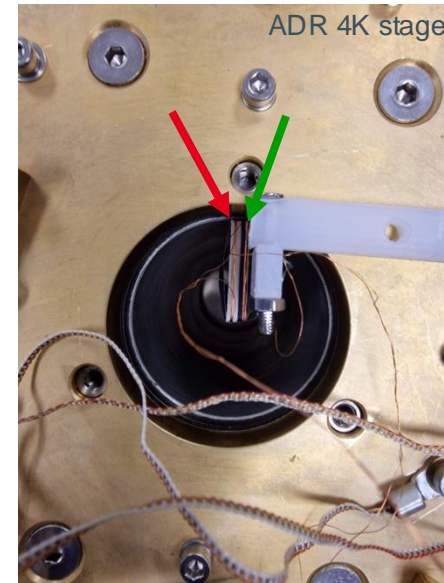
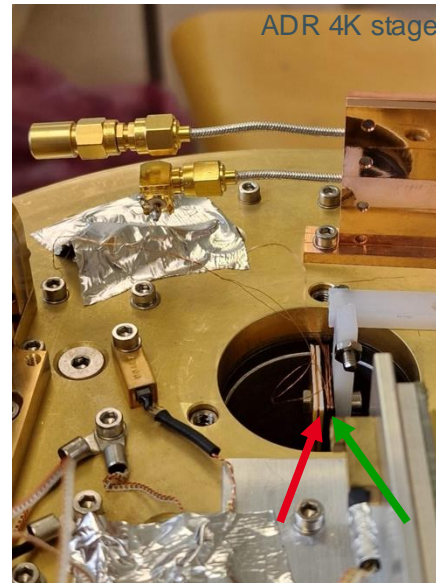
- Installation of an additional **external antenna** next to the ADR, measuring together with the pick-up probe channel & at the same frequency band to reject any incoming as well as **self-created EMI/EMC**.

 see slide 14

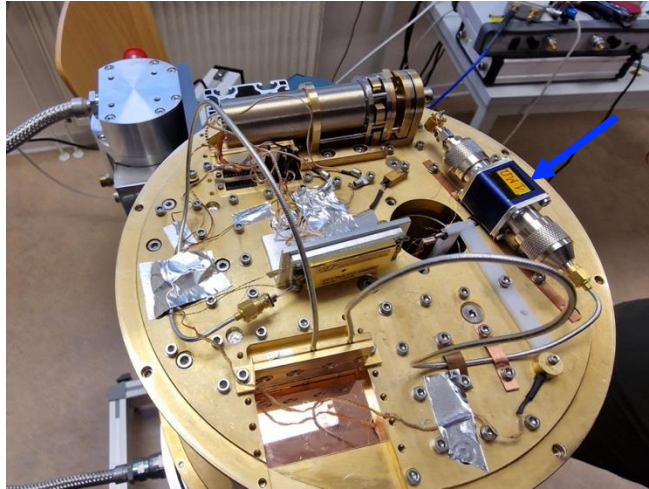


## WISPLC Prototype – Calibration

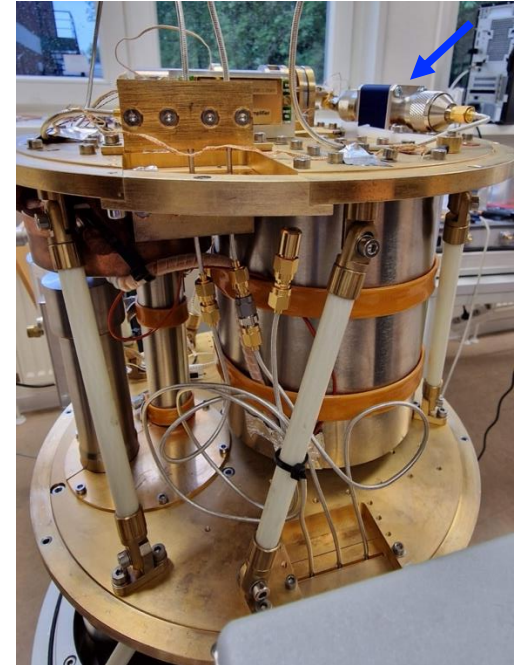
- Installation of a secondary similar Cu **injection loop** parallel to the **pickup loop** for injected signal coupling via mutual inductance.
- Synthetic signal injections for calibration and verification of the data acquisition procedure.



## WISPLC Prototype – Calibration

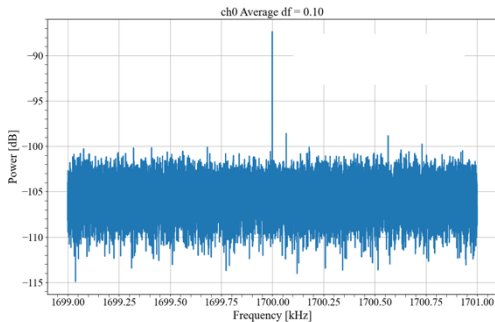


1 MOhm resistor placed in series to transform the injected voltage source into current source.



# WISPLC Prototype – Calibration

- Sweeping from 0 - 10 MHz with a spectrum analyzer at -30 dBm in data-taking conditions.
- As expected, with the LNA and voltage detection setup, we have **increased sensitivity with increasing frequency.**

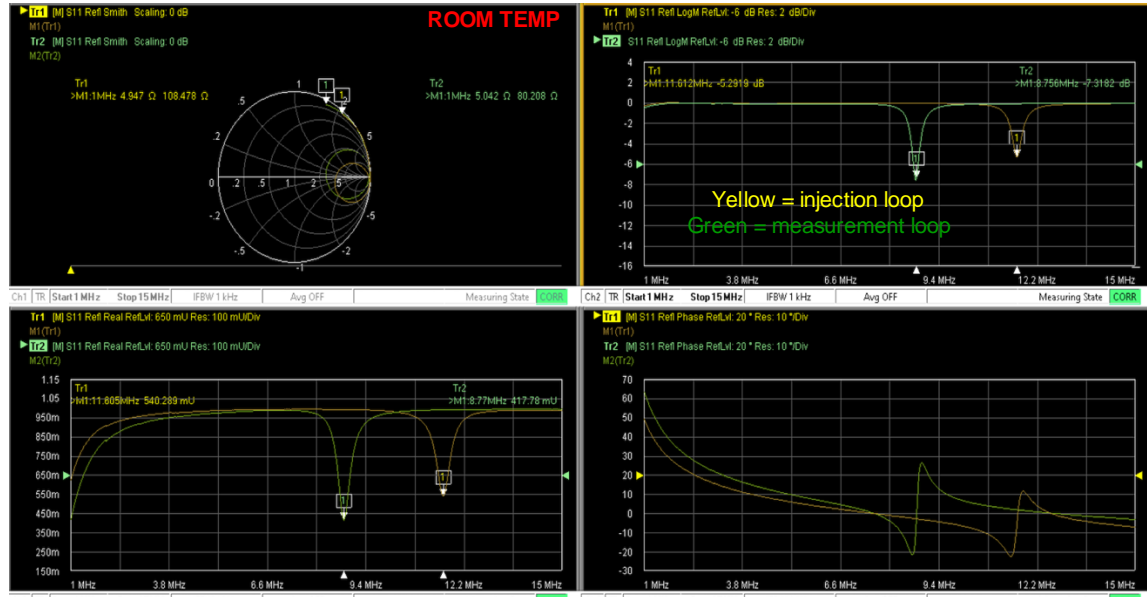


+ Hardware-injected CW signals for DAQ sanity check.



# WISPLC Prototype – Characterization

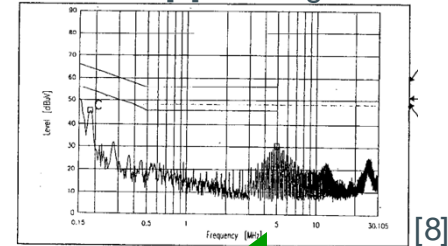
- Impedance & inductance measurement @ room temp + data-taking conditions.
  - Expected values (@ room temp):  $Z_r = 5.5 \text{ Ohm}$   $L=20 \mu\text{H}$
  - Measured values:  $Z_r = 5 \text{ Ohm}$   $L=13 \mu\text{H}$
- Loop inductive up to 10 MHz @ 4K + 6T.
- Similar values for both injection and measurement loops



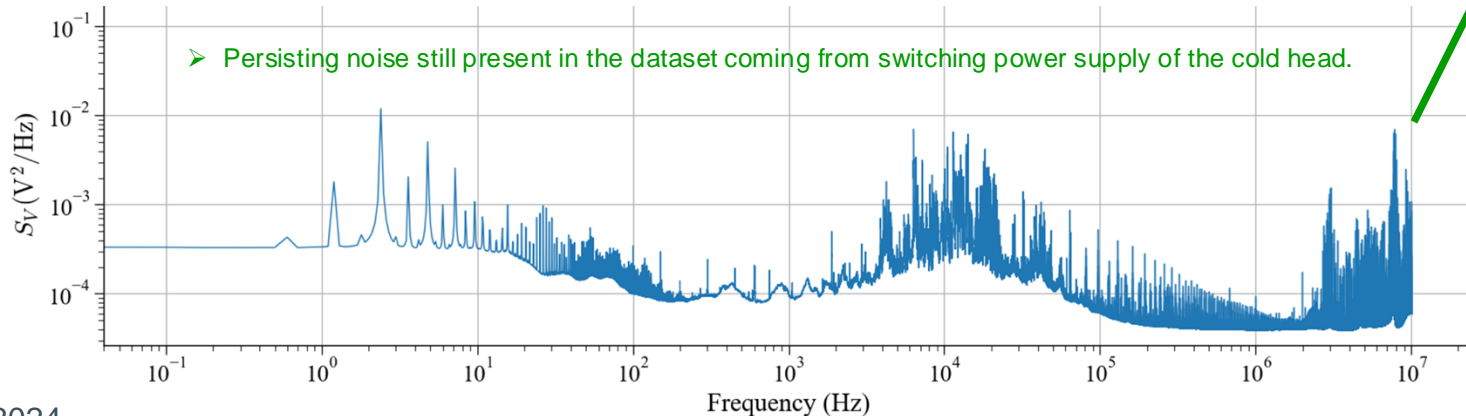
# Data Acquisition Results

- Measured for 84 h with  $B = 6T \rightarrow$  for axion signal search.
- Measured for 48 h with  $B = 3 T \rightarrow$  for EMI/EMC signal elimination.
- Measured for 24 h with  $B = 0 T \rightarrow$  for EMI/EMC signal elimination.
- Measured for 48 h with external probe  $\rightarrow$  for EMI/EMC signal elimination

See also [9] for mitigation

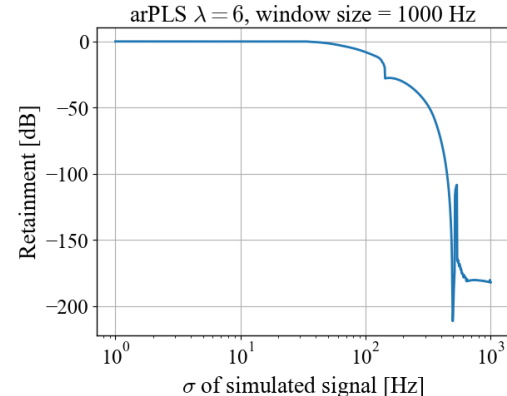
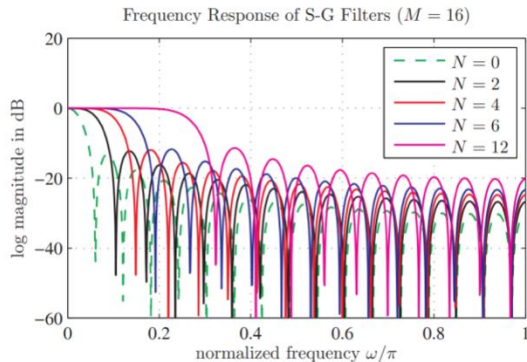


ENS5011-B,ENS5022-Bの限度値はVCCI Class Bの限度値と同じ  
Limits of ENS5011-B and ENS5022-B are same as its VCCI class B.

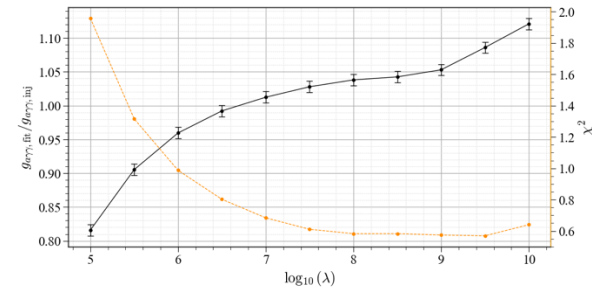


# Data Analysis – Background subtraction

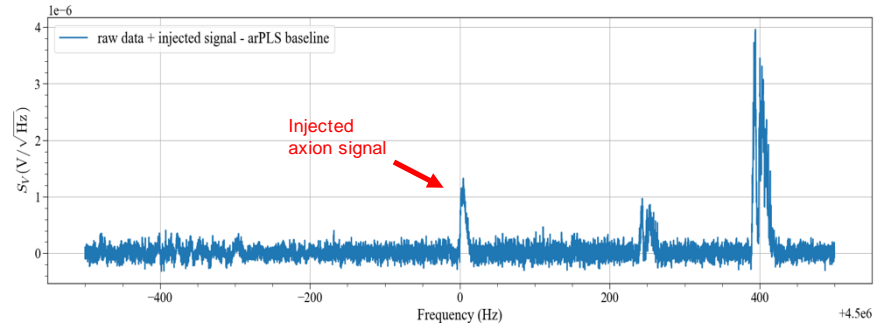
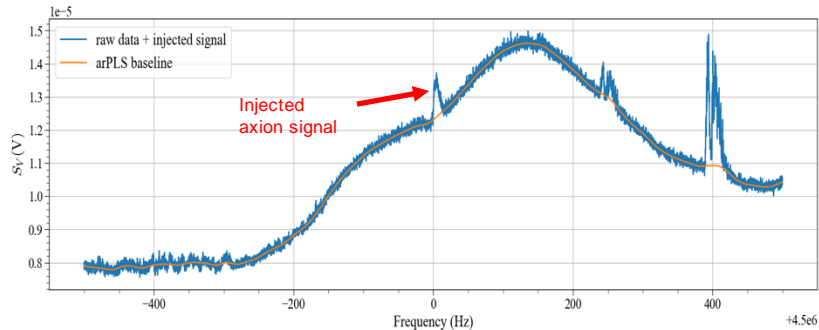
- Use of the asymmetrically-reweighted-Penalized-Least-Squares-Smoothing (arPLS) filter [7] instead of the Savitsky-Golay (SG) due strong EMI/EMC parasites distorting the spectrum shape.
- arPLS filter originally introduced for Raman Spectroscopy.
- SG not suitable for broadband searches due to limited attenuation in the stopband region (see also K. Ozbozduan's talk + poster).



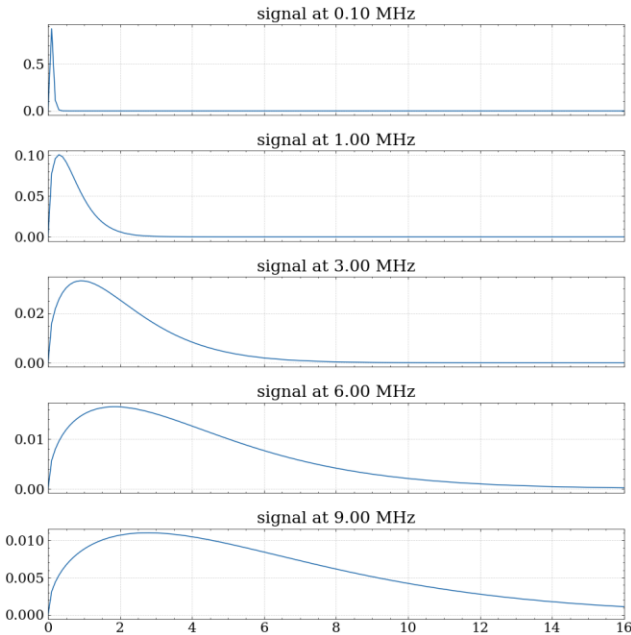
# Data Analysis – Background subtraction



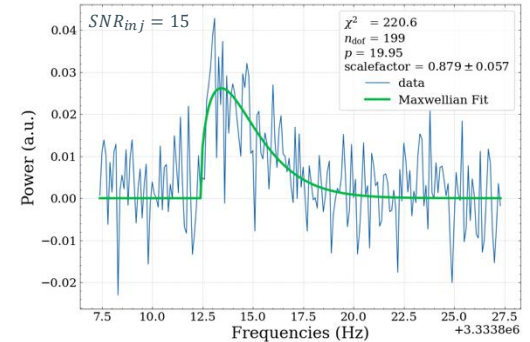
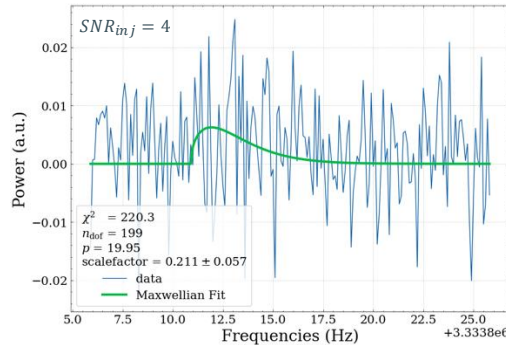
- Optimization of the smoothing parameter  $\lambda$  via Monte-Carlo simulations in order to have the minimum  $\chi^2$ , and the correct axion-photon coupling.



# Data Analysis – Axion signal expectation



- **Varying axion linewidth** from  $\sim 0.1$  Hz to 10 Hz for WISPLC useable 0.1 MHz – 10 MHz frequency range.
- Selected FFT RBW: **0.1 Hz**.
- **Dynamic  $\lambda$**  on arPLS filter for background fitting based on frequency.
- **Blind signal injections** for verification of the analysis procedure.



# Data Analysis – Axion signal search

Signal elimination through the following procedure:

1. Appearance of a signal in the **external probe** dataset.
2. Incompatibility with expected **Maxwellian shape** and/or better linear fit.
3. Appearance of a signal in the  **$B = 0T$**  dataset.
4. Incorrect scaling of a signal in the  **$B = 3T$**  dataset.
5. Incorrect scaling of a signal with **time** (requires re-running of FFT on existing time-domain data).

Signal characterization procedure underway!



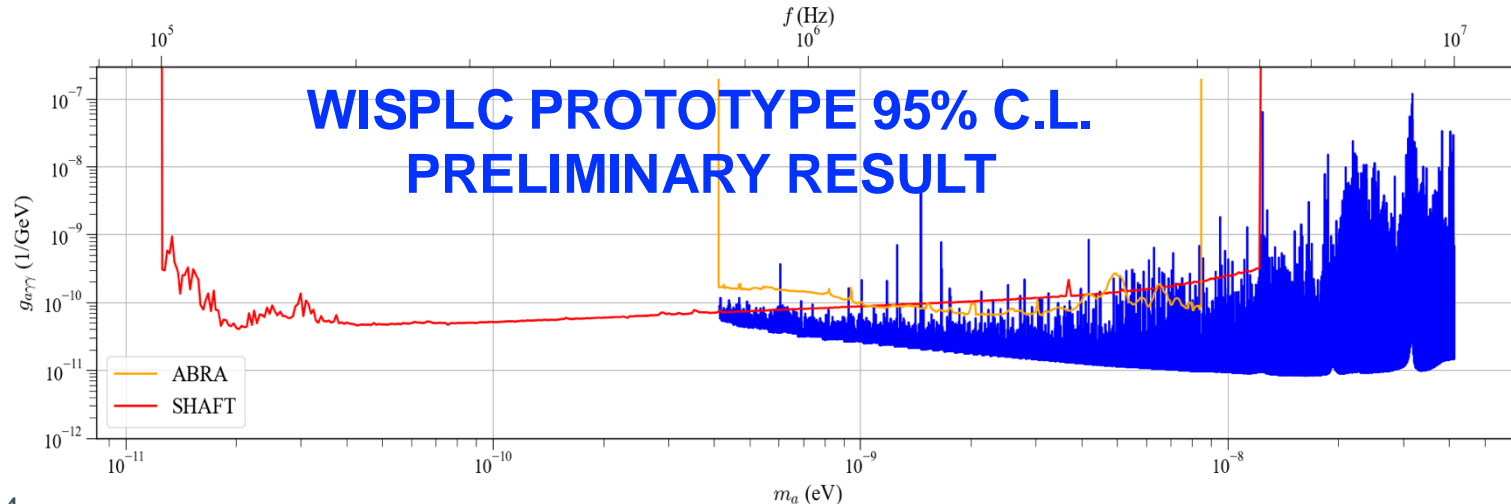
**Stay tuned!!**

# Data Analysis – Exclusion plot

- Assuming no Axion/ALP signal is present in the collected dataset:

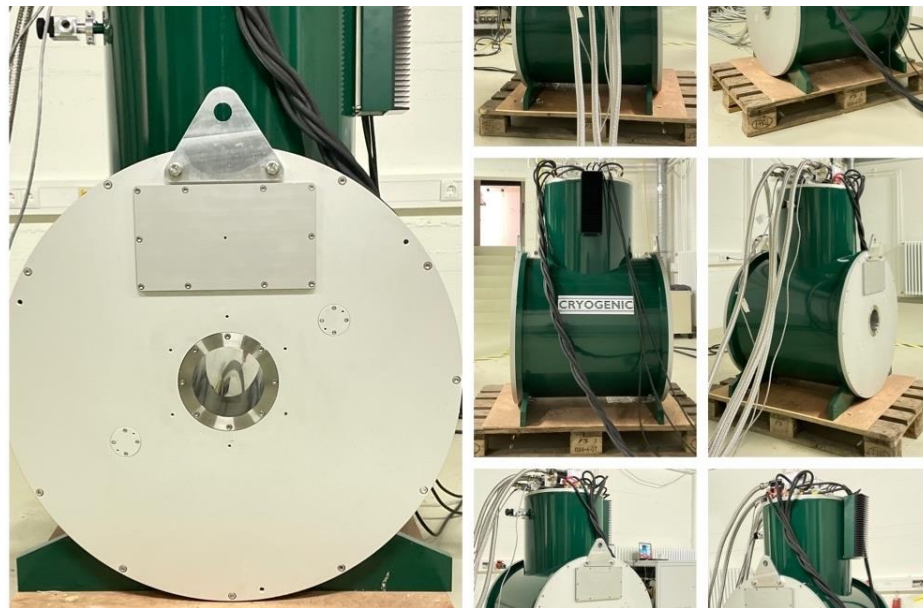


$$g_{a\gamma\gamma} = \frac{\text{SNR } \sigma_{\Phi} (t\tau_a)^{-1/4}}{BV_B \sqrt{2\rho_{\text{DM}}}} = \frac{\text{SNR } \sigma_V (t\tau_a)^{-1/4}}{m_a G N_{\text{loop}} BV_B \sqrt{2\rho_{\text{DM}}}}$$



## Future steps

- ❖ **Publish** current physics results.
- ❖ Replace cold head switching DC power supply with a linear one or use copper mesh on supply line [8] to **reduce self-imposed noise**.
- ❖ Modify loop geometry and wire thickness to increase the inductive behavior of the pickup loop to **higher frequencies**.
- ❖ Introduction of a tuned capacitor in series with the loop for measurement under the **resonant scheme**.
- ❖ Implementation of WISPLC in our **14 T warm-bore magnet** for increased sensitivity.
- ❖ **GW and transient signal search** in the broadband mode.



**Thanks for your attention!**

**Find out more about the cluster:  
[www.qu.uni-hamburg.de](http://www.qu.uni-hamburg.de)**



## References

- (1) R. D. Peccei, H. R. Quinn, Constraints imposed by CP conservation in the presence of pseudoparticles, Phys. Rev. 16, 1791–1797, (1977), <https://doi.org/10.1103/PhysRevD.16.1791>
- (2) Sokolov, A.V., Ringwald, A. Photophilic hadronic axion from heavy magnetic monopoles, J. High Energ. Phys. 2021, 123, (2021), [https://doi.org/10.1007/JHEP06\(2021\)123](https://doi.org/10.1007/JHEP06(2021)123)
- (3) L. d. Luzio et al., Dark matter from an even lighter QCD axion: trapped misalignment, J. Cosmol. Astropart. Phys. 10, 001, (2021), <https://doi.org/10.1088/1475-7516/2021/10/001>
- (4) P. Sikivie, Experimental Tests of the "Invisible" Axion, Phys. Rev. Lett. 51, 1415, (1983), <https://doi.org/10.1103/PhysRevLett.51.1415>
- (5) Z. Zhang, D. Hors, O. Ghosh, Search for dark matter with an LC circuit, Phys. Rev. D., 106, 023003, (2022), <https://doi.org/10.1103/PhysRevD.106.023003>
- (6) F. Bajjali et al., First results from BRASS-p broadband searches for hidden photon dark matter, JCAP08, 077, (2023), <https://doi.org/10.1088/1475-7516/2023/08/077>
- (7) S.J. Baek et al., Baseline correction using asymmetrically reweighted penalized least squares smoothing, Analyst, 140, 250, (2015), <https://doi.org/10.1039/C4AN01061B>
- (8) [https://product.tdk.com/en/search/power/switching-power/ac-dc-converter/info?part\\_no=JWS50-24](https://product.tdk.com/en/search/power/switching-power/ac-dc-converter/info?part_no=JWS50-24)
- (9) M. J. Eshraghi, M. Cho, J. M. Kim and I. Sasada, Conducted EMI Reduction on the Pulse Tube Cryocooler, IEEE Transactions on Magnetics, vol. 45, no. 6, pp. 2754-2757, (2009), <https://doi.org/10.1109/TMAG.2009.2020548>